Asociación Argentina
de Mecánica Computacional

Mecánica Computacional Vol XXXIII, págs. 371-385 (artículo completo)
Graciela Bertolino, Mariano Cantero, Mario Storti y Federico Teruel (Eds.)
San Carlos de Bariloche, 23-26 Setiembre 2014

ASSESSMENT OF NUMERICAL TECHNIQUES FOR MICRO-DROP FLUID MECHANICS

Roberto F. Ausas[a], Santiago Marquez Damian[b], Felipe Montefusculo[c] and Gustavo C. Buscaglia[c]

[a]*IBM Research Brazil, São Paulo, SP, Brazil,*

[b]*CIMEC-CONICET, Santa Fé, Argentina,*

[c]*Instituto de Ciências Matemáticas e de Computação, Universidade de São Paulo, São Carlos, SP, Brazil,*

Keywords: Droplet sedimentation, Two-phase flows, Surface Tension, Parasitic currents.

Abstract. Are currently available CFD techniques able to model the motion of a submilimiter-scale liquid drop falling in another (quiescent) liquid? In this work we define a very simple two-dimensional test: An initially circular drop of water of diameter 0.1 mm is placed at the center of a square box (size 0.6 mm) filled with oil (relative density 0.8). The goal is to compute the fall of the drop towards the bottom of the box, which would take several seconds based on typical terminal velocities found in the problem. It seems easy, doesn't it? We have tested several CFD techniques on this problem: FOAM (two available VOF-based methods within FOAM's platform), GERRIS (free software from Popinet's group), level-set finite elements (interface capturing) and finally ALE finite elements (interface tracking). The aim is to illustrate on the serious limitations this methodologies have to accurately and efficiently track the dropet's trajectory.

1 INTRODUCTION

The study of sedimentation of water droplets in oil is of great interest for the petroleum industry (Frising et al., 2006). Crude oil is seldom produced alone. In majority of cases the oil is produced along with water. Due to the presence of active agents in the oil, a water-in-oil emulsion is produced, i.e., an emulsion with oil being the continuous phase and water the dispersed one. Several factors can influence the formation of such emulsions, such as the flow through the porous medium or the turbulence mixing at pipes and valves (Barnea and Mizrahi, 1975). After extraction the two phases are separated which is usually acomplished by using the so called gravity settlers where two important phenomena are observed: *droplet coalescence* and *droplet sedimentation*. Both are interesting and challenging phenomena to deal with from a computational standpoint. The former because it involves merging of interfaces and therefore requires robust numerical techniques to handle topological changes of the fluid phases. The latter, which is the main interest here, although simple at a first glance, also presents challenges because it requires tracking of the droplet trajectory for several seconds until it settles down at the bottom of the separator. The diameter of droplets of interest for these applications are in the *submilimiter* scale with values near 0.1mm. Under these conditions the flow is highly dominated by viscous and surface tension effects and droplets remain spherical along their sedimentation.

State-of-the-art CFD techniques for two-phase flows dominated by surface tension in this operating range suffer from severe time step restrictions (Galusinski and Vigneaux, 2008) and/or from the so called parasitic currents (Scardovelli and Zaleski, 1999) if coarse meshes or low order approximations are used, in which case simulation results may end up being totally meaningless. Refining the time step and the mesh render numerical simulations for the whole history of sedimentation, even for a single droplet, extremely costly. The aim of this article is precisely to illustrate on this point by using several numerical techniques which include, various VOF solvers (Weller et al., 1998; Popinet, 2009; Márquez Damián, 2013), a finite element level set method as proposed in Ausas (2010) and an Arbitrary Lagrangian Eulerian method as proposed in Montefuscolo (2012). The simulation results show the behavior and robustness of the different methodologies to predict the evolution of a single submilimiter water droplet in oil.

By means of outline, after this introduction, the equations and non-dimensional parameters governing the sedimentation of droplets are presented. Next, the different numerical methodologies considered to discretize the problem are suscintly recalled and numerical results from each one are shown to illustrate on their limitations for different time step and mesh resolutions. Finally, some conclusions are drawn.

2 GOVERNING EQUATIONS

All the numerical methodologies used in this work to assess the sedimentation of the droplet implement the resolution of the mathematical problem describe in this section. We consider two-phase immiscible Newtonian flows. The fluid domain Ω is divided into a "plus" $(+)$ region and a "minus" $(-)$ region by a closed (smooth) interface Γ as shown in figure 1, such that

$$\Omega \;=\; \Omega^{+}(t) \,\cup\, \Gamma(t) \,\cup\, \Omega^{-}(t). \tag{1}$$

The density ρ and viscosity μ are assumed homogeneous and constant within each region, namely

$$(\rho(\mathbf{x},t),\mu(\mathbf{x},t)) = \begin{cases} (\rho^{+},\mu^{+}) & \text{if } \mathbf{x}\in\Omega^{+}(t) \\ (\rho^{-},\mu^{-}) & \text{if } \mathbf{x}\in\Omega^{-}(t) \end{cases} \tag{2}$$

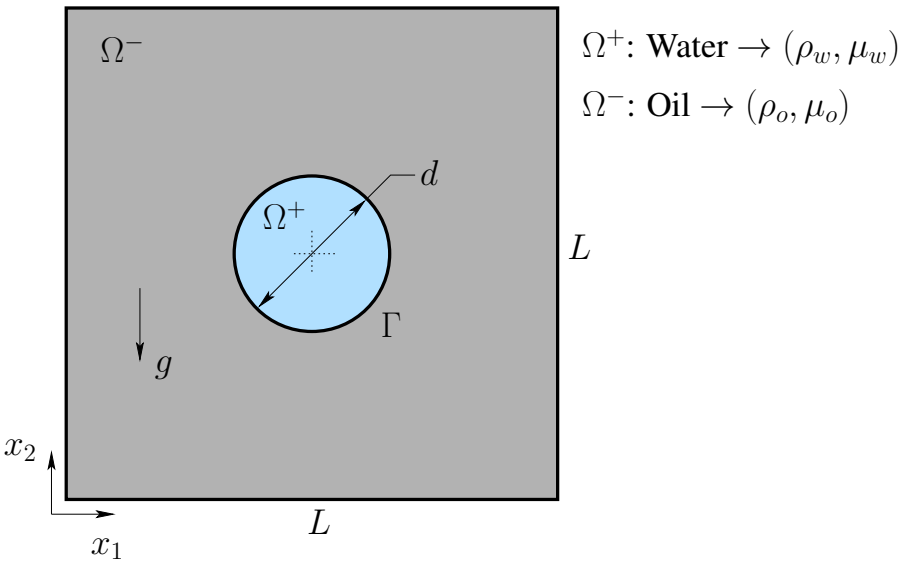

Figure 1: Schematic diagram of the problem setting.

On each region we need to solve the dynamical equilibrium equations, i.e.,

$$\rho\left(\partial_t \mathbf{u} + \mathbf{u}\cdot\nabla\mathbf{u}\right) - \nabla\cdot\boldsymbol{\tau} + \nabla p = -\rho\, g\, \hat{\mathbf{e}}_2 \quad \text{in} \quad \Omega^+(t)\cup\Omega^-(t) \tag{3}$$

where $\mathbf{u}$ is the velocity field, p is the pressure field, $-g\,\hat{\mathbf{e}}_2$ is the gravitational force and $\boldsymbol{\tau} = \mu\left(\nabla\mathbf{u} + \nabla^T\mathbf{u}\right)$ is the stress tensor. The incompressibility restriction reads

$$\nabla\cdot\mathbf{u} = 0 \quad \text{in} \quad \Omega^+(t)\cup\Omega^-(t) \tag{4}$$

In this work we also consider the following initial and boundary conditions

$$\left\{\begin{array}{rcll} \mathbf{u}(\mathbf{x}, t=0) & = & 0 & \mathbf{x}\in \Omega^+(t)\cup\Omega^-(t) \\ \mathbf{u}(\mathbf{x}, t) & = & 0 & \mathbf{x}\in \partial\Omega \end{array}\right. \tag{5}$$

Interface conditions

Important for this problem are the jump conditions at the interface Γ. For capillary interfaces, the jump conditions for velocity and stresses on the interface read

$$\left\{\begin{array}{rcll} [\![\mathbf{u}]\!] & = & 0 & \text{on } \Gamma \\ [\![\boldsymbol{\tau}\cdot\check{\mathbf{n}}]\!] & = & \sigma\,\kappa\,\check{\mathbf{n}} - \nabla_\Gamma\sigma & \text{on } \Gamma \end{array}\right. \tag{6}$$

In which $[\![\cdot]\!]$ represents the jump of any quantity at Γ, σ is the surface tension coefficient, κ is the mean curvature of Γ and $\check{\mathbf{n}}$ is the normal vector to Γ pointing towards Ω^+. The first condition implies that incompressibility is satisfied at the interface. The second condition incorporates the dynamical effects at Γ. Here, σ is assumed constant and uniform along Γ for the sake of simplicity and therefore we neglect Marangoni effects coming from its surface gradient $\nabla_\Gamma\sigma$. These effects are generally due to chemical or thermal gradients. The variables that are expected to be discontinuous at Γ are thus the pressure field and the velocity gradient. For more details see Buscaglia and Ausas (2012).

The interface conditions appear naturally in a variational formulation of the problem which is well suited for the finite element methods used later on. An alternative equivalent approach useful for discretization in other frameworks, is to consider the surface tension force as a singular force at the interface, i.e.,

$$\mathbf{F}_\sigma = \delta_\Gamma \sigma \, \kappa \, \check{\mathbf{n}} \quad \text{on } \Gamma \tag{7}$$

This is the approach followed in the VOF formulation presented in the following section. The Dirac distribution δ_Γ can be further regularized for discretization purposes leading to different formulations in turn.

2.1 Sedimentation velocity

In this work our aim is to assess different numerical methodologies to simulate the sedimentation of a single water droplet in oil as shown in figure 1. For the sake of simplicity, we consider a two dimensional (planar) setting and therefore study the sedimentation of "large cylinders". The behavior of droplets in different flow regimes is studied in the classical work of Clift et al. (2005). Here it is reasonable to assume that surface tension effects dominate the problem and the droplet remains circular along its evolution. Since the Reynolds number is also expected to be small, a simple estimation based on Stokes' flow gives the following expression for the sedimentation velocity

$$U_s = \sqrt{\frac{g\, d\, \pi}{C_d} \frac{\rho_w - \rho_o}{\rho_o}}, \tag{8}$$

where ρ_w and ρ_o are the densities of water and oil respectively, d is the droplet's diameter, and C_d is the drag coefficient which for low Reynolds number is roughly proportional to $\sim 1/\mathrm{Re}$, yielding (see Perry (1950))

$$U_s = \frac{(\rho_w - \rho_o)\, g\, d^2}{18\, \mu_o}, \tag{9}$$

where μ_o is the oil viscosity (the continuous phase). Different estimations can be made for the Drag coefficient as proposed in Finn (1953)

$$C_d = \frac{8\,\pi}{[\frac{1}{2} - 0.577 - \ln(\mathrm{Re}/8)]\,\mathrm{Re}}, \tag{10}$$

but an iterative procedure is then needed to compute U_s. The velocity U_s is used to effectively compute the non-dimensional parameters in the next subsection and confirm the assumptions already made.

2.2 Non-dimensional groups

Dimensional analysis on the governing equations leads to five non-dimensional parameters for this problem: the Reynolds number, the Froude Number, the Weber number and the ratio between densities ρ_o/ρ_w and viscosities μ_o/μ_w. However, some additional numbers are usually used in the literature to characterize these flows. The parameters of interest here are the Reynolds number, the capillary number Ca, the Eötvos number Eo and the Laplace number La. They can be all obtained as combinations of the formers and are defined as

$$\begin{aligned} \mathrm{Re} &= \frac{\rho\, U\, d}{\mu}, & \mathrm{Ca} &= \frac{\mu\, U}{\sigma} \\ \mathrm{Eo} &= \frac{\Delta\rho\, g\, d^2}{\sigma}, & \mathrm{La} &= \frac{\sigma\, \rho\, d}{\mu^2} \end{aligned} \tag{11}$$

The characteristic velocity is chosen as the terminal or sedimentation velocity U_s previously introduced. The physical parameters adopted for the numerical simulations are summarized in table 1. These values correspond to water droplets in oil. Notice the large viscosity ratio μ_o/μ_w of 300 considered. Using the aforementioned rough estimation for the drag coefficient the sedimentation velocity results in

$$U_s \approx 3.7 \times 10^{-6}\,\text{m/s}, \tag{12}$$

finally yielding

$$\begin{aligned} \text{Re} &= 1.16 \times 10^{-6}, \quad & \text{Ca} &= 6.54 \times 10^{-5} \\ \text{Eo} &= 10^{-3}, & \text{La} &= 1.78 \times 10^{-2} \end{aligned} \tag{13}$$

Under these conditions, the flow is clearly in the Stokes regime and dominated by surface tension and viscosity.

Table 1: Physical parameters adopted for the sedimentation of a water droplet in oil.

Parameter	Symbol	Value [SI]
Droplet diameter	d	0.0001 m
Domain size	L	0.0006 m
Gravity acceleration	g	10 m/s^2
Dispersed phase (Water Droplet):		
Density	ρ_w	1000 kg/m^3
Viscosity	μ_w	0.001 Pa s
Continuous phase (Oil):		
Density	ρ_o	800 kg/m^3
Viscosity	μ_o	0.3 Pa s
Interface:		
Surface tension coefficient	σ	0.02 kg/s^2

3 NUMERICAL METHODS

3.1 Parasitic currents

Parasitic currents are a consequence of discretization errors in the numerical modeling of capillary flows. They have been extensively discussed in the literature in various numerical settings. References on the subject can be consulted e.g. in Popinet (2009) and Scardovelli and Zaleski (1999). Some numerical techniques, specially those based on an implicit representation of the interface non-conforming with the edges/faces of the underlying mesh where the flow problem is being solved, are particularly affected by them. Examples of these techniques are the well known level set and VOF methodologies used later on in this work. Several details of the discretization affect the strenght and form of these parasitic currents. Although, a complete review of this topic is out of the scope of the article, we may mention:

- mesh quality and resolution (Deshpande et al., 2012; Lafaurie et al., 1993; Harvie et al., 2006);
- size of time step (Galusinski and Vigneaux, 2008);

- treatment of discontinuous variables close to Γ, such as the pressure and the velocity gradient (Ausas et al., 2012; Idelsohn et al., 2010);
- accuracy in the discrete representation of Γ and computation of normal and curvature fields (Gross and Reusken, 2007; Cummins et al., 2005; Marchandise et al., 2007),

The behavior of different numerical methods with respect to these factors can vary a lot. As an example, in VOF methods the magnitude of spurious velocities can even increase with mesh refinement as reported in Deshpande et al. (2012). Other classes of methods, as those based on an explicit Lagrangian representation of the interface, such as the Arbirtrary Lagrangian Eulerian (ALE) method may exhibit better behaviors as we show later on.

In this work we assess three different classes of methods to solve the sedimentation of the droplet. In the first place, the VOF method, based on a finite volume discretization of the problem. In the second place, an equal order finite element level set method in the form proposed by Ausas (2010). Finally, a finite element ALE method proposed by Montefuscolo (2012). Here, without entering into all the details, we suscintly recall the main ingredients involved on each of them. Prior to this we briefly discuss the time step restrictions that are expected in these problems.

3.2 Time step restrictions

We consider here numerical schemes in which velocity and pressure are solved with a fixed interface geometry and then geometry is updated with the last computed velocity. These are called staggered schemes for which a time step restriction is expected. According to Galusinski and Vigneaux (2008) the time step Δt needs to satisfy the following limiting criterion for stability

$$\Delta t \leq \Delta t_{\text{lim}} \approx \frac{1}{2}\left\{ C_2 \frac{h\mu}{\sigma} + \sqrt{(C_2 \frac{h\mu}{\sigma})^2 + 4\, C_1 \frac{\rho h^3}{\sigma}} \right\}, \tag{14}$$

where h is the element size and C_1 and C_2 are constants depending on the specific method but not on the mesh size and the physical parameters of the problem. For instance, in Deshpande et al. (2012) the authors assess the behavior of `interFoam` solver (Weller et al., 1998) and experimentally find values of 0.01 and 10 for C_1 and C_2 respectively. One would expect that a reasonable value for the mesh size h in our problem be of the order of $d/10$, meaning that a single droplet in a 3D simulation is resolved with 1000 discretization points. This would be an affordable quantity if the aim is at simulating for instance 1000 droplets. The numerical values for viscosity and density considered in table 1 yield $\Delta t_{\text{lim}} \approx 10^{-5}$ s (at worst). According to the terminal velocity previously computed of 3.7×10^{-6} m/s, the droplet requires ~ 80s to settle down at the bottom of the computational domain, which means that 8 millon time steps are needded to complete the simulation!. Of course, this restriction can be improved for some of the formulations by using a semi-implicit scheme as proposed by Bänsch (2001) or an implicit scheme as done in Buscaglia and Ausas (2012); Ausas et al. (2009) to deal with the surface tension force.

Now, we describe the main features of the numerical schemes to be tested. Again, we emphatize that a staggered scheme is used in which $\mathbf{u}$ and p are first solved with a fixed interface, and then Γ is transported with the last computed $\mathbf{u}$.

VOF - Finite volume methods

In the Volume of Fluid (VOF) method initially proposed by Hirt and Nichols (1981) the incompressible Navier-Stokes equations (3) are solved by using a density and viscosity defined by

$$\begin{aligned} \mu &= \alpha\,\mu^- + (1-\alpha)\,\mu^+, \\ \rho &= \alpha\,\rho^- + (1-\alpha)\,\rho^+, \end{aligned} \tag{15}$$

α being the volume fraction of the primary phase, i.e., it is a scalar field that assumes values equal to 1 at those cells completely in Ω^-, 0 at those cells completely in Ω^+ and varies between 0 and 1 in those cells on the interface. The advection of α is governed by the following equation in conservative form

$$\partial_t \alpha + \nabla\cdot(\alpha\,\mathbf{u}) + \nabla\cdot[\alpha\,(1-\alpha)\,\mathbf{v}_r] = 0, \tag{16}$$

where $\mathbf{v}_r$ is the relative velocity between the two phases. Theoretically, this velocity should be zero, however, in some implementations it is retained to add some compressibility at the interface, which actually turns the problem non-linear. In this work several formulations or implementations are tested, specifically, the `InterFoam` solver of Weller et al. (1998), a derived solver called `interDyMFoam`, both in the free software suite OpenFOAM® and the also publicly available `Gerris` software proposed by Popinet (2003). Some ingredients common to all the aforementioned VOF implementations that were adopted in this work are:

- Discretization of the computational domain into finite volume quadrilateral cells.
- Cell-centered finite volume method.
- Derivation of the PISO method for pressure-velocity coupling.
- Geometric properties and surface tension force computed based on the volume fraction without regularizations.
- Multidimensional Universal Limiter with Explicit Solution (used in FOAM implementations, see Deshpande et al. (2012); Márquez Damián (2013)) and TVD scheme in Gerris to solve the advection equation.

Regarding the computation of the surface tension force mentioned in the itemized list above, at each cell, the normal vector and curvature are computed based on α as (Brackbill et al., 1992)

$$\check{\mathbf{n}} = \frac{\nabla\alpha}{\parallel\nabla\alpha\parallel}, \quad \kappa = -\nabla\cdot\nabla\left(\frac{\nabla\alpha}{\parallel\nabla\alpha\parallel}\right) \tag{17}$$

yielding the following form for the surface tension force

$$\mathbf{F}_\sigma = \sigma\,\kappa\,\check{\mathbf{n}} \tag{18}$$

Level set - Finite element method

In the level set method (Osher and Sethian, 1988) the interface is defined as the zero set of a scalar function $\phi(\mathbf{x},t)$, i.e.,

$$\Gamma = \{\mathbf{x}\in\Omega,\ \phi(\mathbf{x}) = 0\}, \tag{19}$$

this function should satisfy the condition

$$\nabla\phi(\mathbf{x}) \neq 0 \quad \mathbf{x}\in\Gamma, \tag{20}$$

so as the normal to Γ is well defined and given by

$$\check{\mathbf{n}}(\mathbf{x}) = \frac{\nabla\phi(\mathbf{x})}{\| \nabla\phi(\mathbf{x}) \|} \quad \mathbf{x} \in \Gamma \tag{21}$$

The level set function and implicitly Γ, are transported by the velocity field $\mathbf{u}$ that follows after solving the Navier-Stokes equations (3). This transport is done by means of solving the hyperbolic advection equation

$$\partial_t\phi + \mathbf{u} \cdot \nabla\phi = 0 \quad \text{in } \Omega, t > 0 \tag{22}$$

where the initial condition $\phi(\mathbf{x}, 0) = \phi_0(\mathbf{x})$ is defined according to the initial position of the interface. Also, appropriate Dirichlet boundary conditions are needed at the inflow boundaries if present. A thorough description of the complete formulation and details adopted here can be found elsewhere (see Ausas (2010)). The finite element method is adopted for spatial discretization, whose main ingredients are summarized below.

- Discretization of the computational domain into triangles.
- Equal order formulation to solve the Navier-Stokes equations (3) using linear elements for velocity and pressure and algebraic subgrid scale method for stabilization (see e.g. (Codina, 2001; Hughes et al., 1986)).
- SUPG formulation to solve the transport equation (22) with P_1 elements for the level set function.
- First order temporal accuracy.
- Modified pressure space proposed in Ausas et al. (2010) to capture discontinuities in the pressure field.
- Laplace-Beltrami treatment of the surface tension force.

Using standard P_1 elements for the level set function implies that the reconstructed interface is elementwise planar. In the Laplace-Beltrami approach, the curvature computation is avoided by means of integrating by parts along Γ (Buscaglia and Ausas, 2012).

ALE method

In an ALE formulation Hughes et al. (1981); Baiges et al. (2010); Rabier and Medale (2003) the interface between the two fluids is represented by the edges (in 2D) or faces (in 3D) of the mesh in which the flow problem is being solved. For the particular problem we have at hand, this formulation is expected to be accurate and robust to follow the falling droplet. In the ALE method the finite element partition moves with time. Each nodal position is a function of time that is denoted by $\mathbf{x}^j(t)$. The nodal velocity can be defined as

$$\mathbf{v}^j(t) \doteq \frac{d\mathbf{x}^j(t)}{dt}, \tag{23}$$

index j running over the nodes of the finite element partition. The velocity field is approximated as

$$\mathbf{u}_h = \sum_j N^j(\mathbf{x}, t)\, \mathbf{u}^j(t), \quad N^j(\cdot, t)\, \mathbf{e}_\alpha \in W_h(t) \tag{24}$$

where $\mathbf{e}_\alpha,\ \alpha = 1, \ldots, d$ is the canonical basis, and $\mathbf{u}^j(t)$ are the nodal velocity values. In (24) $W_h(t) \subset (H^1(\Omega(t)))^d$ is a finite dimensional space that depends parametrically on time. A key point in the derivation of the ALE formulation is the following identity

$$\partial_t \mathbf{u}_h = \sum_j N^j \frac{d\mathbf{u}^j}{dt} - (\mathbf{v}_h \cdot \nabla)\mathbf{u}_h \tag{25}$$

which inserted into a classical spatial discretization of the variational form of (3) yields a differential algebraic equation system to which any temporal discretization scheme can be applied. The formulation adopted here is presented with details in Montefuscolo (2012). The main ingredients of the implementation are

- Discretization of the computational domain into triangles.
- Equal order formulation to solve the Navier-Stokes equations (3) using linear elements for velocity and pressure and algebraic subgrid scale method for stabilization.
- Discontinuos elements for the pressure field at the interface.
- Linear elements for geometry interpolation.
- First order temporal accuracy.
- Elasticity-like problem for the mesh velocity equation.
- Laplace-Beltrami treatment of the surface tension force.

As noticed, many features of the approximation are shared with the finite element level set methodology presented above.

4 NUMERICAL RESULTS

In this section we present results from each numerical methodology to illustrate on their limitations. The numerical values adopted and the corresponding non-dimensional parameters are the ones given in section 2.2. Similar numerical studies using Eulerian and Lagrangian formulations are presented for instance in Bertaki et al. (2010) and Bäumler et al. (2011), however, in none of these articles the authors address the *submiliter* scale as done here.

Before passing to the results, some comments are in order. For both finite element based formulations, namely, the level set and the ALE methods, simulations are carried out for different grid resolutions. The central region of the computational domain is refined so as to have mesh resolutions h equal to $d/10$, $d/20$ and $d/40$, while a coarser mesh is generated far a way from the region of interest. For the VOF simulations, uniform and locally refined meshes only near the interface are used. This allows us to save some computational time and assess the behavior of the different formulations with respect to grid resolution. Simulations runs until one second of physical time when possible. Although this is a short time compared to the total one needed for complete sedimentation, and the steady state velocity may not be even reached for some of the simulations, we have found this sufficient to characterize the behavior of the numerical schemes. Finally, we also report on the center of mass position and velocity computed as

$$\mathbf{r}_{\mathrm{cm}}(t) = \frac{1}{\mathrm{meas}(\Omega^+(t))}\int_{\Omega^+(t)} \mathbf{x}\, d\Omega, \qquad \mathbf{u}_{\mathrm{cm}}(t) = \frac{1}{\mathrm{meas}(\Omega^+(t))}\int_{\Omega^+(t)} \mathbf{u}(\mathbf{x}, t)\, d\Omega \tag{26}$$

rembembering the value previously estimated for the sedimentation velocity is 0.0037 mm/s.

4.1 VOF results

In this section we present results corresponding to different VOF formulations: `interFoam`, `interDyMFoam` and `Gerris`. Other formulations also tested as `iInterFoam` showed very similar results or did not succeed in completing a significant part of the total simulation time and therefore are not shown here for the sake of brevity. The finite volume meshes used in the simulations are shown in figure 2. For `interFoam` two meshes are considered: a regular one with a cell size $\Delta x = d/10$ and a adaptively locally refined one with up to three levels of refinement obtained by uniform cell splitting near the droplet's interface. In `Gerris` code the grid is also adaptively refined as the simulation proceeds similarly to `interDyMFoam`. The initial grid is always consisting of an uniform regular grid with $\Delta x = d/10$. The time step Δt used in simulations are 10^{-6}s for the uniform mesh used by `interFoam` and 10^{-7}s for the refined grids used by `interDyMFoam` and `Gerris`. For the finer meshes, simulations are computationally very demanding and we were able to report results only for the different times indicated. The velocity fields are shown in figure 3. As observed the strenght of parasitic currents is totally polluting the results for `interFoam` and `interDyMFoam`. The droplet remains essentially at its initial position during most part of the simulation and for this reason the plot is not shown. Further mesh and time step refinements do not solve the problem. For `Gerris`, on the other hand, results start to improve with the level of refinement considered. This is due to the improved treatment for the curvature field by means of the so called height functions used in this implementation. The droplet did not attain the terminal velocity but the flow pattern is clearly symmetric as expected. These results already show serious limitations of some of the VOF implementations, even when very fine meshes are used.

Using `Gerris` software, with the adaptevely refined grid and time step, the complete sedimentation can be simulated in approximately 67 days on a 4-core desktop computer with i7 processor at 2.9 GHz.

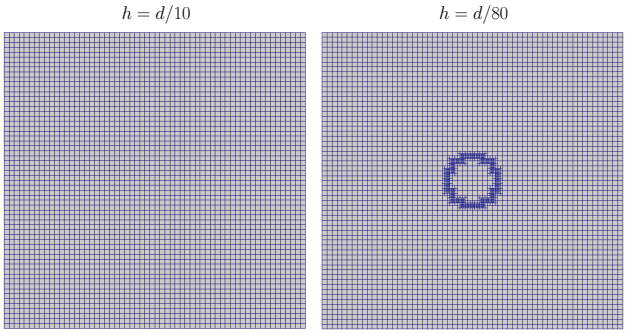

Figure 2: Finite volume meshes used for the VOF simulations.

4.2 Level set results

The finite element meshes built for the level set simulations are displayed in figure 4. As previously mentioned they are finer in the region of intereset, being this more than sufficient to simulate 1 s of time. The time step Δt used in simulations is 10^{-4}s for the first mesh, 5×10^{-5}s for the second one and 2.5×10^{-5}s for finest one. Remember the modified pressure space is being used to capture the discontinuous behavior of p at the interface, however, this is not enough to avoid the nocive effect of the parasitic currents as shown in figure 5 where the velocity

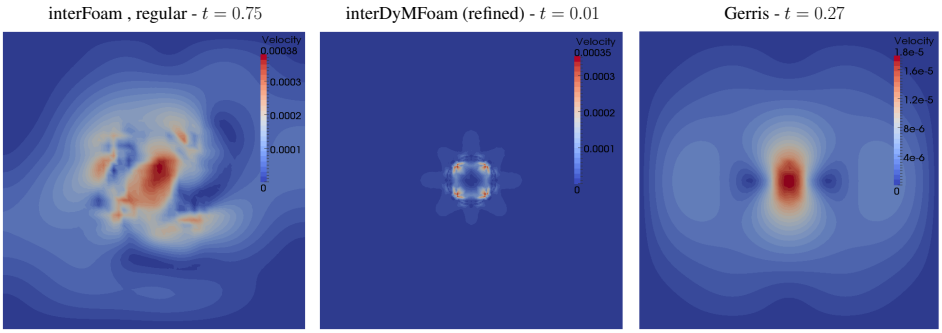

Figure 3: Velocity field (in m/s) obtained with the VOF formulation for the different implementations at the final simulated time for each case.

field at $t = 1$ is plotted. The maximum of the colour scale in these figures is dictated by the maximum parasitic current which sometimes is limited to few elements, hindering the fact that most of the droplet phase is moving at the same velocity. This is particularly the case for the third refinement level and to some extent for the second refinement. Figure 6 shows the droplet's vertical position and velocity as a function of time for the three meshes. Results start to be acceptable for the third refinement in which the size of the parasitic currents is sufficiently reduced being their effect limited to a very small region and/or for small periods of time. For the sake of clarity, in these plots only a fraction of the total number of simulated points is shown. The poorest results are obtained for the first refinement (red dots) for which the strenght of the spurious velocities completely pollutes the droplet's trajectory.

For the finest mesh (consisting of 14406 triangular elements), using a time step $\Delta t = 2.5 \times 10^{-5}$, the complete sedimentation can be simulated in approximately 15 days on a 4-core desktop computer with i7 processor at 2.9 GHz.

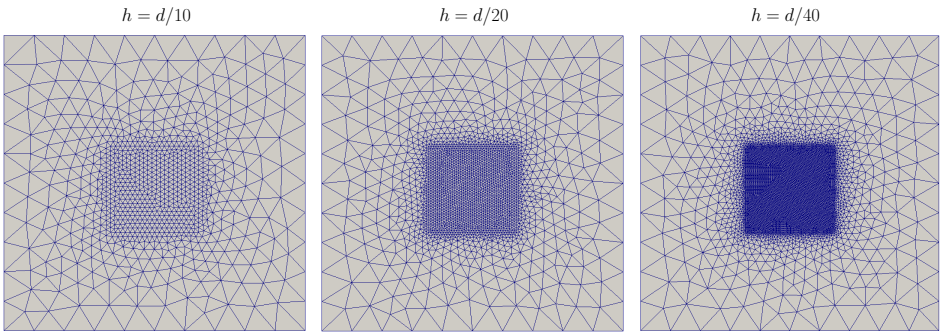

Figure 4: Finite element meshes used for the level set simulations.

4.3 ALE results

The finite element meshes built to compute the flow with the ALE formulation are shown in figure 7. A finer region in the central part of the computational domain is also considered, although a smoother transition from fine to coarse elements is used. The droplet interface is coincident with the element edges as can be notice by zooming in at these plots. The corresponding velocity fields are shown in figure 8. The time step Δt used in simulations is 10^{-4}s for the first mesh and 10^{-5}s for the rest of the meshes. The superior behavior of this formulation

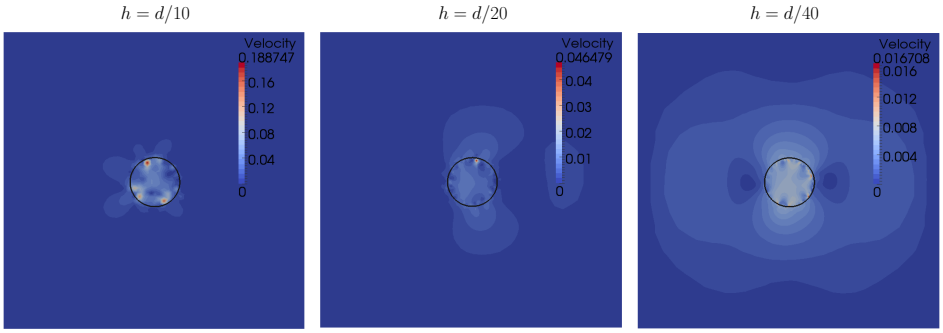

Figure 5: Velocity field (in mm/s) obtained with the level set formulation on the different meshes at $t = 1$.

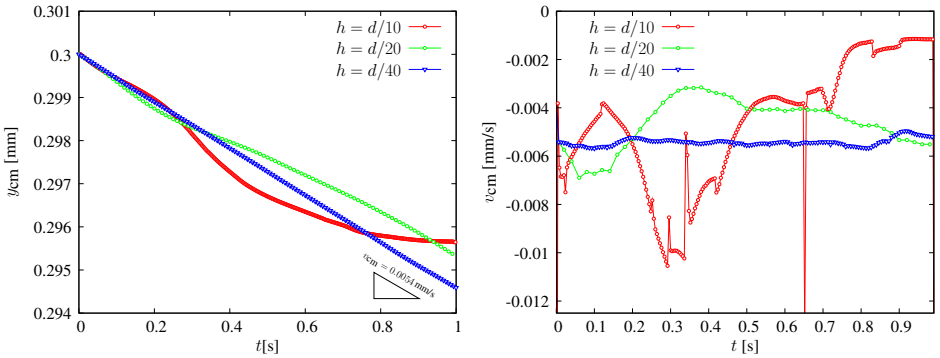

Figure 6: Droplet's center of mass position (left) and velocity (right) as a function of time obtained with the level set formulation for the different meshes.

as compared to previous ones is quite evident. This is also seen by plotting the evolution of the center of mass position and velocity as a function of time (see figure 9). As observed in figure 9, the droplet does not attain the terminal value of the sedimentation velocity at the end of the simulation, and the time needed to do so seems to be quite dependent on mesh resolution. The main limitations observed are related to the size of the time step needed in principle for stability if the staggered scheme is used, although this can be partially relaxed.

For the coarsest mesh (consisting of 1516 triangular elements) for which results are already reasonably accurate, using a time step $\Delta t = 10^{-4}$, the complete sedimentation can be simulated in approximately 30 days on a 4-core desktop computer with i7 processor at 2.9 GHz.

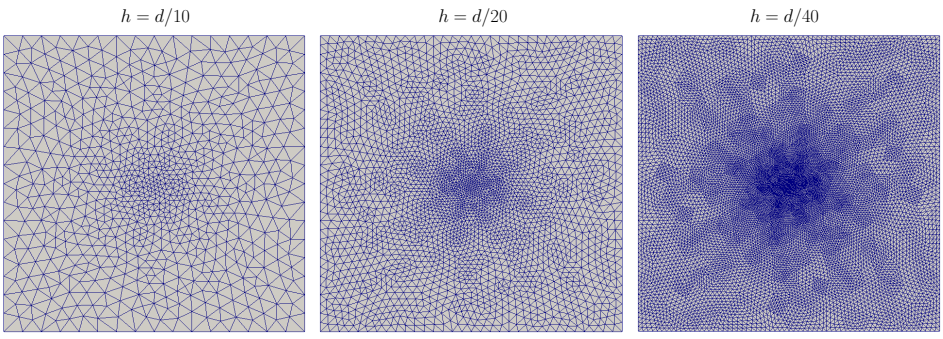

Figure 7: Finite element meshes used for the ALE simulations.

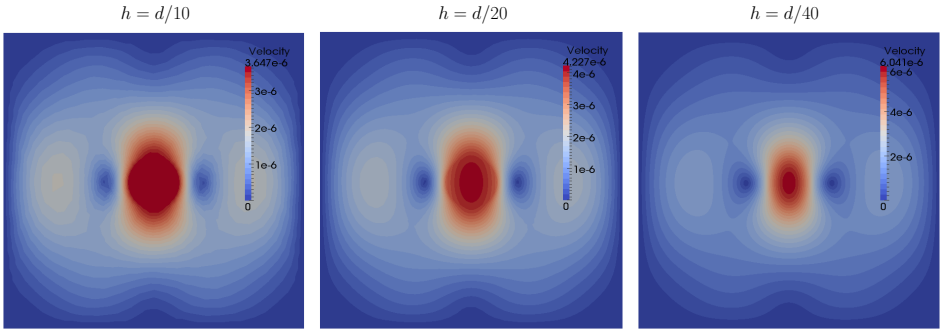

Figure 8: Velocity field (in m/s) obtained with the ALE formulation on the different meshes at $t = 1$.

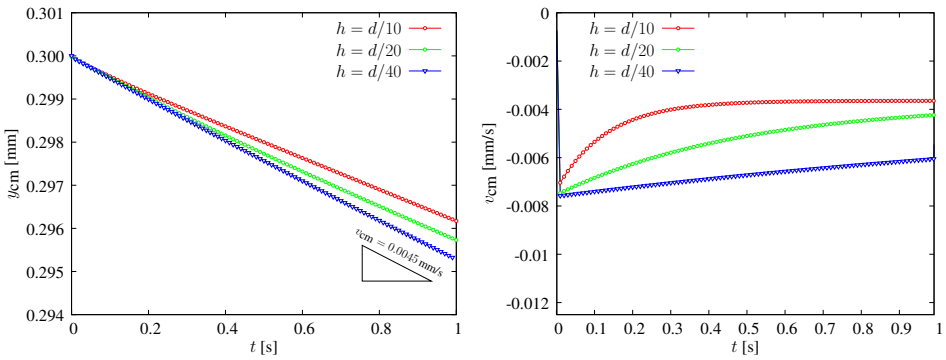

Figure 9: Droplet's center of mass position (left) and velocity (right) as a function of time obtained with the ALE formulation for the different meshes.

5 CONCLUSIONS

We have shown the behavior of three different classes of numerical methods for two-phase capillary flows to assess a relevant problem for the oil industry related to the sedimentation of submilimiter water droplets in oil. It has been shown that there exist serious limitations of such methods to efficiently solve the problem: millons of very short time steps are needed to follow the whole history of sedimentation when staggered schemes are used and/or very fine meshes becomes necessary to reduce the size and extent of parasitic currents. If the final goal is the simulation of real systems involving thousands of 3D droplets, these are extremely limiting factors. For the VOF method, the only implementation that seems to be sufficiently accurate for this problem is the one used in the publicly available software `Gerris`. In some of the implementations tested, including some commercial ones, the simulation even reached the final time, or the droplet's behavior was totally polluted by the parasitic currents with desastrous consequences. For the level set method, the linear interpolation used for interface representation becomes a very limiting factor to as regards accuracy. Results start to be reasonably accurate for moderately refined meshes. In this case, as well as for the ALE approach, adding implicitness to the formulation is relatively easy and certainly mitigates the time step restriction issue as has been verified although not reported here for the sake of brevity. As expected, the ALE formulation outperformed the rest of the methodologies with respect to accuracy for a given mesh resolution.

6 ACKNOWLEDGMENTS

The authors gratefully acknowledge the financial support received from FAPESP (Grants. no. 2012/14481-8 and 2012/04560-8) and from the Brazilian National Research and Technology Council (CNPq). SMD gratefully acknowledge the financial support received from Universidad Nacional del Litoral and CEPID-CeMEAI.

REFERENCES

Ausas R. *Simulación Numérica en Flujo de dos Fases Inmiscibles con aplicaciones en Lubricación Hidrodinámica*. Ph.D. thesis, Engineering, Instituto Balseiro, 2010.

Ausas R.F., Buscaglia G.C., and Dari E.A. Una formulación monolítica para flujos a superficie libre con cálculo numérico del jacobiano. *Serie Mécanica Computacional*, XXVIII::1391–1407, 2009.

Ausas R.F., Buscaglia G.C., and Idelsohn S.R. A new enrichment space for the treatment of discontinuous pressures in multi-fluid flows. *International Journal for Numerical Methods in Fluids*, 70:829–850, 2012.

Ausas R.F., Sousa F.S., and Buscaglia G.C. An improved finite element space for discontinuous pressures. *Computer Methods in Applied Mechanics and Engineering*, 199:1019 – 1031, 2010.

Baiges J., Codina R., and Coppola-Owen H. The fixed-mesh ALE approach for the numerical simulation of floating solids. *International Journal for Numerical Methods in Fluids*, 2010.

Bänsch E. Finite element discretization of the Navier–Stokes equation with a free capillary surface. *Numer. Math.*, 88:203–235, 2001.

Barnea E. and Mizrahi J. Separation mechanism of liquid-liquid dispersions in a deep-layer gravity settler: Part I-The structure of the dispersed band. *Trans. Inst. Chem. Eng.*, 53:61–69, 1975.

Bäumler K., Wegener M., Paschedag A., and Bänsch E. Drop rise velocities and fluid dynamic behavior in standard test systems for liquid/liquid extraction - experimental and numerical investigations. *Chemical Engineering Science*, 66:426–439, 2011.

Bertaki E., Gross S., Grande J., Fortmeier O., Reusken A., and Pfenning A. Validated simulation of droplet sedimentation with finite-element and level-set methods. *Chemical Engineering Science*, 65:2037–2051, 2010.

Brackbill J., Kothe D., and Zemach C. A continuum method for modeling surface tension. *J. Comput. Phys.*, 100(2):335–354, 1992.

Buscaglia G.C. and Ausas R.F. Variational formulations for surface tension, capillarity and wetting. *Computer Methods in Applied Mechanics and Engineering*, 70:829–850, 2012.

Clift R., Grace J., and Weber M. *Bubbles, Drops and Particles*. Dover publications, 2005.

Codina R. A stabilized finite element method for generalized stationary incompressible flows. *Comput. Methods Appl. Mech. Engrg.*, 190:2681–2706, 2001.

Cummins S., Francois M., and Kothe D. Estimating curvature from volume fraction. *Computers and Structures*, 83:425–434, 2005.

Deshpande S., Anumolu L., and Trujillo M. Evaluating the performance of the two-phase flow solver interfoam. *Computational Science & Discovery*, 5(1):014016, 2012.

Finn R. Determination of the drag on a cylinder at low reynolds numbers. *J. Applied Physics*, 24(6):771–773, 1953.

Frising A., Noïka C., and Dalmazzonea C. The liquid/liquid sedimentation process: From droplet coalescence to technologically enhanced water/oil emulsion gravity separators: A

review. *Journal of Dispersion Science and Technology*, 27(7):1035–1057, 2006.

Galusinski C. and Vigneaux P. On stability condition for bifluid flows with surface tension: application to microfluidics. *J. Comput. Phys.*, 227:6140âĂŞ–6164, 2008.

Gross S. and Reusken A. Finite element discretization error analysis of a surface tension force in two-phase incompressible flows. *SIAM J. Numer. Anal.*, 45:1679–1700, 2007.

Harvie D., Davidson M., and Rudman M. An analysis of parasitic current generation in volume of fluid simulations. *Applied Mathematical Modelling*, 30(10):1056–1066, 2006.

Hirt C. and Nichols H. Volume of fluid (VOF) methods for the dynamics of free boundaries. *Applied Numerical Mathematics*, 39:201–225, 1981.

Hughes T., Franca L., and Balestra M. A new finite element formulation for computational fluid dynamics: V. circumventing the babuška-brezzi condition. a stable petrov-galerkin formulation of the Stokes problem accommodating equal-order interpolations. *Comput. Methods Appl. Mech. Engrg.*, 59:85–99, 1986.

Hughes T., Liu W., and Zimmermann T. Lagrangian–Eulerian finite element formulation for incompressible viscous flows. *Comput. Meth. Appl. Mech. Engrg.*, 29:329–349, 1981.

Idelsohn S., Mier-Torrecilla M., Nigro N., and Oñate E. On the analysis of heterogeneous fluids with jumps in the viscosity using a discontinuous pressure field. *Computational Mechanics*, 46(1):115–124, 2010.

Lafaurie B., Nardone C., Scardovelli R., Zaleski S., and Zanetti G. Modelling merging and fragmentation in multiphase flows with surfer. *J. Comput. Phys.*, 113(1):134–147, 1993.

Marchandise E., Geuzaine P., Chevaugeon N., and Remacle J.F. A stabilized finite element method using a discontinuous level set approach for the computation of bubble dynamics. *J. Comput. Phys.*, 225:949–974, 2007.

Márquez Damián S. *An extended mixture model for the simultaneous treatment of short and long scale interfaces*. Ph.D. thesis, FICH, Universidad Nacional del Litoral, Santa Fe, Argentina, 2013.

Montefuscolo F. *Métodos numéricos para escoamentos com linhas de contato dinâmicas.* Master's Thesis, Instituto de Ciências Matemáticas e de Computação, Universidade de São Paulo, São Carlos, 2012.

Osher S. and Sethian J. Front propagating with curvature-dependent speed: algorithms based on Hamilton-Jacobi formulations. *J. Comput. Phys.*, 79:12–49, 1988.

Perry J. *Chemical Engineers Handbook, 3rd Edition*. McGraw Hill, 1950.

Popinet S. Gerris: a tree-based adaptive solver for the incompressible euler equations in complex geometries. *J. Comput. Phys.*, 190(2):572–600, 2003.

Popinet S. An accurate adaptive solver for surface-tension-driven interfacial flows. *Journal of Computational Physics*, 228(16):5838–5866, 2009.

Rabier S. and Medale M. Computation of free-surface flows with a projection FEM in a moving mesh framework. *Comput. Methods Appl. Mech. Engrg.*, 192(41):4703–4721, 2003.

Scardovelli R. and Zaleski S. Direct numerical simulation of free-surface and interfacial flow. *Annual Review of Fluid Mechanics*, 31(1):567–603, 1999.

Weller H., Tabor G., Jasak H., and Fureby C. A tensorial approach to computational continuum mechanics using object-oriented techniques. *Computer in Physics*, 12(6):620–631, 1998.